



**HAL**  
open science

## **SPICAM Climatology of Aerosol Vertical Distribution through UV Occultations**

Anni Määttänen, Constantino Listowski, Franck Montmessin, L. Maltagliati,  
L. Joly, Aurélie Reberac, Jean-Loup Bertaux

► **To cite this version:**

Anni Määttänen, Constantino Listowski, Franck Montmessin, L. Maltagliati, L. Joly, et al.. SPI-CAM Climatology of Aerosol Vertical Distribution through UV Occultations. The Fifth International Workshop on the Mars Atmosphere: Modelling and Observations, Jan 2014, Oxford, United Kingdom. pp.id. 1405. hal-01062208

**HAL Id: hal-01062208**

**<https://hal.science/hal-01062208>**

Submitted on 6 Apr 2015

**HAL** is a multi-disciplinary open access archive for the deposit and dissemination of scientific research documents, whether they are published or not. The documents may come from teaching and research institutions in France or abroad, or from public or private research centers.

L'archive ouverte pluridisciplinaire **HAL**, est destinée au dépôt et à la diffusion de documents scientifiques de niveau recherche, publiés ou non, émanant des établissements d'enseignement et de recherche français ou étrangers, des laboratoires publics ou privés.

# SPICAM CLIMATOLOGY OF AEROSOL VERTICAL DISTRIBUTION THROUGH UV OCCULTATIONS.

**A. Määttänen, C. Listowski, F. Montmessin, LATMOS, Université Versailles St Quentin, Centre National de la Recherche Scientifique, Guyancourt, France (anni.maattanen@latmos.ipsl.fr), L. Maltagliati, LESIA, Observatoire de Paris, Meudon, France, L. Joly, Groupe de Spectrométrie Moléculaire et Atmosphérique GSMA, Université de Reims, Reims, France, A. Reberac, J.-L. Bertaux, LATMOS, Université Versailles St Quentin, Centre National de la Recherche Scientifique, Guyancourt, France.**

## Introduction

We will present observations of aerosol profiles derived from MEx/SPICAM solar occultations in the ultraviolet ([1]) completed with UV stellar occultations. This dataset allows, as described by [2] for stellar occultations, the retrieval of vertical profiles of the abundance of gaseous species ( $\text{CO}_2$ ,  $\text{O}_3$ ), aerosol optical depth in the UV, and the Ångström coefficient, which can be, through some hypotheses, related to particle size. The first solar occultation results were presented by [3]. Since then, the SPICAM technical team has provided new corrections for the data, giving access to previously unused orbits, and new geometry files. A data analysis code, including a correction for mechanical oscillations induced by the MARSIS radar antennae, has been developed and used in the analysis. We have analysed all solar occultations of adequate quality between orbit numbers 0-10000 (Mars Years 27-30) spanning 4 MY with a good seasonal and spatial coverage. The results reveal the dust haze near the surface, and detached layers (possibly clouds) at high altitudes. We will present a global overview of the results and some specific cases of interest from the several hundreds of occultations analysed, and complete the solar occultation dataset with a comparison to the UV stellar occultations.

The abstract is based on [1] where the solar occultation results have been published.

## Dataset

SPICAM (SPectroscopie pour l'Investigation des Caractéristiques Atmosphériques de Mars) is observing Mars in the ultraviolet (118–320 nm) and in the near infrared (1–1.7  $\mu\text{m}$ ) ranges. [4] describes the instrument and the observation techniques in detail. In the occultation mode, the UV channel allows to infer the vertical distribution of  $\text{CO}_2$ ,  $\text{O}_3$ , and aerosols. We are focusing here on the UV solar occultation dataset of about 650 profiles, and we are also including over 800 UV stellar occultations mainly from MY27-28 (with some observations in MY29-30) to achieve a better overall coverage in latitude and  $L_s$ . We also wish to compare the results of the two datasets that mainly differ only by the local time of observation acquisition (solar occultations

at the terminator, stellar occultations during the night). The calculated transmission spectra are fitted with the Beer-Lambert law, which takes into account extinction by gaseous species and aerosols. Aerosol extinction is modeled with the so-called alpha-model, providing access to the Ångström coefficient, which depends on the size of the aerosols. However, we can not determine the composition of the particles through the observations, which can make the size determination dependent on the assumed composition. Inversely, for very large Ångström coefficients only ice composition is possible, but again there is no way to discriminate between  $\text{H}_2\text{O}$  and  $\text{CO}_2$  ices.

## Hazetops

The so-called hazetop (the altitude where the slant opacity drops to  $\tau = 1$  from the higher near-surface values) gives information about the vertical extent of the low-lying, well-mixed continuum of aerosols (haze) that prevails near the surface of Mars. This haze should be composed of dust outside the polar regions: the polar hoods are formed of fairly low-lying clouds. The source of the dust haze is lifting from the surface and mixing through atmospheric convection. The hazetop can thus give some information on the atmospheric activity and its variations.

Figure 1 shows the variations of the hazetop as a function of latitude and season. In this figure all the observations are mixed regardless of the year of acquisition. The stellar occultations included in the figure cover a larger (unpublished) dataset than just those analyzed by [2].

In general, higher hazetop values are observed at warmer seasons and regions, i.e., near the equator, and in the southern hemisphere during southern spring and summer ( $L_s = 180\text{--}360^\circ$ ). Here convection acts more efficiently and the general circulation is stronger: aerosols can be lifted to and maintained at higher altitudes. This happens in particular around the perihelion ( $L_s = 220\text{--}300^\circ$ ) where dust storms occur more often ([5]). Seasonal temperature changes modulate the cloud formation level as well. Consequently cloud formation regulates the dust haze extent through scavenging of dust particles and sedimentation to the lower atmosphere.

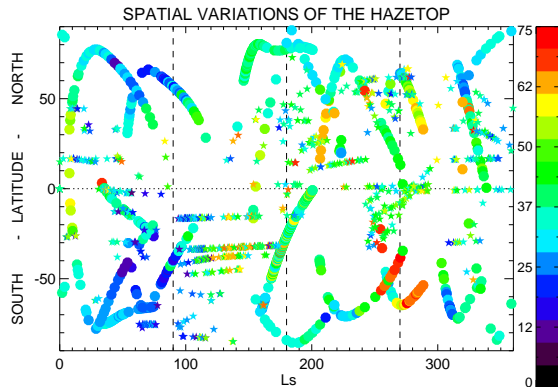


Figure 1: The whole hazetop dataset as a function of latitude and season. The circles and stars represent solar and stellar occultations, respectively. The color scale gives the hazetop altitude.

### Detached layers

In almost half (48%) of the analyzed solar occultation profiles, and in more than two thirds (70%) of the stellar occultation profiles, the slant optical depth has a clear local maximum that we can identify as an aerosol layer (including multiple layers, 13% of observed layers in solar occultations). These layers are observed at all latitudes and seasons throughout the analysed dataset (Figure 2). In most cases, these maxima are found at high altitudes

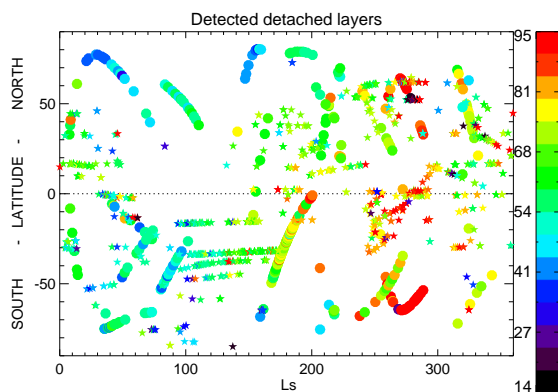


Figure 2: The detached layer dataset as a function of latitude and season. The circles and stars represent solar and stellar occultations, respectively. The color scale gives the detached layer altitude.

above the near-surface haze, but clear layer structures are as well found within the near-surface haze. It should be kept in mind that the slant optical depth includes information from several altitudes along the line of sight. Thus certain effects may be due to the geometry of the observations. For example, a layer observed within the

haze, may be a result of the projection of a layer in the fore or background of the local vertical. Our discussion here concentrates mainly on the more frequent cases of layers above the haze (i.e., high-altitude detached layers). A systematic investigation was performed to detect these clearly-defined atmospheric structures. A detached layer may consist of ice condensates or it might be a dust plume. However, in the occultation mode, we cannot spectrally distinguish between these cases. In contrary to what [2] found, such structures are not limited to mid-southern latitudes in our data.

### Seasonal behavior of hazetop and detached layers

Some interesting phenomena were observed when following the seasonal evolution of the hazetop and the detached layers. Around the northern autumn equinox in MY27 the hazetop altitudes change nearly simultaneously, but in the opposite directions. In the north, the haze remains confined below 40 km after the change, whereas in the south the hazetop altitude increases and high-altitude detached layers are observed very frequently. This might be the first indications of the starting dust storm season in the south. The northern occultations scan the polar regions, showing most probably the development of the polar hood. Here the slant opacities are quite high in the lower atmosphere, and the transition from aerosol-loaded to aerosol-free atmosphere is very sharp.

Observations at the southern spring/summer ( $L_s = 200\text{--}290^\circ$ ) were acquired during two campaigns, at MY 28 and MY29. They include the global dust storm of MY28, and we also should be seeing the early ("pre-season") dust activity in MY29 pointed out by [6]. We can observe seasonal variations of the hazetop in the southern summer through the southern hemisphere parts of the campaigns ( $L_s = 170\text{--}270^\circ$ ) that reveal an increase in hazetop altitudes in the southern midlatitudes as the local spring advances and the circulation becomes more vigorous on average. There is an abrupt increase in the hazetop altitude at around  $L_s = 240^\circ$ . This can also be seen in the detached layers. High-altitude layers are clearly more abundant at this season, with the highest layers of our whole dataset observed during the dust storm.

In the early winter in the southern hemisphere, we have observed a distinct, quite constant, but thin aerosol layer at around 40 km with  $\tau_{aer} < 0.1$  in about 10 consequent profiles ( $L_s = 43\text{--}53^\circ$ ). This layer is detected only in occultations made directly south of the Hellas basin ( $70\text{--}72^\circ\text{S}$ ). This layer stands out from the data since the majority of the detached layers in this season are found in the northern leg of the campaign, and since the shape of the profile and its altitude are very constant. In all the profiles displaying this persistent layer, the Ångström coefficients in the layers are greater than 2.6, indicating

that only ice crystals can explain the wavelength dependence of the opacity. The effective radii of the crystals in the layer are very small, of the order of 100 nm or slightly less, and the smallest crystals are found in range of 50nm. We believe this cloud is related to the forming south polar hood.

### Interannual variations

The seasonal variation of hazetop altitude (for all occultations regardless of latitude, longitude, or Mars Year) can be seen in Fig. 3. The figure reproduces a similar figure of [2], and includes their data and the additional stellar occultation data analyzed later. Fig. 3 reveals

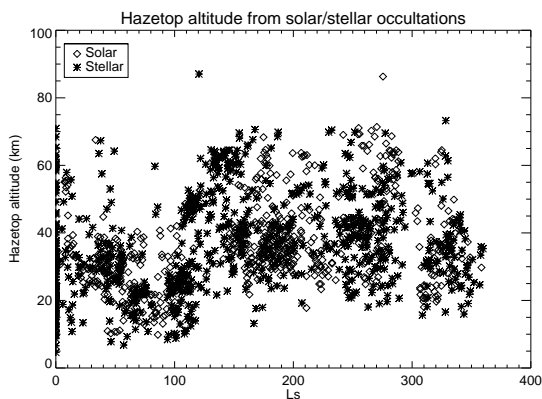


Figure 3: The hazetop altitude as a function of season.

the seasonality in the hazetop altitude, shown already by [2], but with our more extensive dataset the increase in hazetops during the second half of the year is less clear than in [2]: Here we see much larger variability during the southern spring/summer. The most prominent feature of the plot is the minimum at around  $L_s=90^\circ$ . Our observations include the dust storm of MY28 providing the large hazetop altitude variations and large hazetop values in the southern summer. Compared to stellar occultations, the solar occultations span a wider range of latitudes during a given season, inducing more scatter for a given  $L_s$ .

We can now discuss further the inter-annual variability with the help of Figure 1. Two solar occultation observation campaigns were acquired in the southern hemisphere near  $65^\circ\text{S}$  during the same season ( $L_s = 34\text{--}110^\circ$ ), but they account respectively for MY27 and MY29. They display similar average hazetop values in this region and season. Also the MY27 stellar occultations show similar values. It seems that the hazetop follows a quite undisturbed seasonal cycle at this period at mid-to-high southern latitudes since we discover almost the same hazetop altitude two MY apart, and with a global dust storm in between. For these same

solar occultation campaigns, the mean layer altitude of the detached layers in the southern hemisphere shows a very small 4 km difference. However, the layers in MY29 are almost twice as thick (in vertical extent, 11 km) as those of MY27 (6 km), and show higher opacities with respect to the background. This might be the effect of the global dust storm of MY28. The storm has charged the atmosphere full of condensation nuclei, which have had a long-term effect on the microphysical properties of clouds without changing their formation altitude.

The most significant source of inter-annual variability in the solar occultation data is the global dust storm of MY28. We have observations on two campaigns for the southern spring/summer season. If we investigate separately MY28 and MY27, we can mention that the mean hazetop altitude observed only slightly later in season in MY27 is 23 km lower in the southern and 14 km lower in the northern hemisphere than during the dust storm of MY28. This reveals the remarkable vertical extent of the dust advected by the storm. Also the detached layer average altitudes of MY27 are clearly lower (59–61 km), compared to MY28 (77–81 km). Occultations can not be used to define the composition of these layers, but probably the atmosphere is heated strongly by the suspended dust causing the condensation level of water (and consequently the cloud formation level) to be found at higher altitudes.

### Ångström coefficients

The alpha-model used to fit the wavelength dependence of the aerosol extinction gives access to the particle size. However, several assumptions are required before the conversion can be made, and thus unambiguous conclusions are difficult to draw. Thus, we have mainly investigated the vertical variation of the coefficient. We have looked for vertical trends of the coefficient and the particle effective radii in correlation with the opacity profiles in the solar occultation data. It might be expected that in the dust haze the particle radii decrease (Ångström coefficient increases) with increasing altitude simultaneously with a similar trend in opacity. In addition, if the detached layers are ice clouds, one might expect the radii to be larger (smaller Ångström coefficients) than in the surroundings, since the ice crystals form on dust particles. Contrary to the conclusions of [2], in the solar occultation data, we have not always seen this "expected" behavior of increasing coefficient (decreasing particle size) with increasing altitude, nor do we have a systematic decrease (increase in particle size) within the detached layers. Thus it is very difficult to draw conclusions on the behavior of the effective radii in the haze and on the composition of the detached layers. In one exceptional case of the detached layer near Hellas mentioned above, the particles were identified as

## REFERENCES

ice crystals thanks to their large Ångström coefficients.

### Conclusion

The four Martian years of data of SPICAM occultations show that the seasonal behavior of the hazetop follows closely the seasonal variations of the temperature. The highest hazetops are observed at the warm season around the southern summer solstice. Observations during the MY28 dust storm reveal very high hazetops and detached layers. The high northern latitudes in the autumn give the opposite example of very calm vertical distribution with a low hazetop. These data show that the assumption of a well-mixed dust in the lowest atmosphere is not the only option, but that the martian dust vertical distribution is very variable. We observed detached layers in more than half of the analyzed orbits (accounting for both solar and stellar occultations). The highest detached layers are observed during the global dust storm of MY28, but evident single and multiple layers are observed also during other seasons.

The solar occultation dataset can be accessed through the Supplementary Material of the article [1] and the Europlanet IDIS atmospheres node that can be found at <http://www.bdap.ipsl.fr/idis/>.

### References

- [1] Määttänen, A., Listowski, C., Montmessin, F., Maltagliati, L., Reberac, A., Joly, L., Bertaux, J.-L., Apr. 2013. A complete climatology of the aerosol vertical distribution on Mars from MEx/SPICAM UV solar occultations. *Icarus* 223, 892–941.
- [2] Montmessin, F., Quémerais, E., Bertaux, J.-L., Korablev, O., Rannou, P., Lebonnois, S., 2006. Stellar occultations at UV wavelengths by the SPICAM instrument: Retrieval and analysis of Martian haze profiles. *J. Geophys. Res.* 111, E09S09, doi:10.1029/2005JE002662.
- [3] Listowski, C., Määttänen, A., Montmessin, F., Lefèvre, F., Bertaux, J.-L., Feb. 2011. Solar Occultation with SPICAM/UV onboard Mars Express: Retrieving Aerosol and Ozone Profiles. In: Forget, F., Millour, E. (Eds.), *Mars Atmosphere: Modelling and observation*. pp. 191–194.
- [4] Bertaux, J., Korablev, O., Perrier, S., Quémerais, E., Montmessin, F., Leblanc, F., Lebonnois, S., Rannou, P., Lefèvre, F., Forget, F., Fedorova, A., Dimarellis, E., Reberac, A., Fonteyn, D., Chaufray, J. Y., Guibert, S., Oct. 2006. SPICAM on Mars Express: Observing modes and overview of UV spectrometer data and scientific results. *Journal of Geophysical Research (Planets)* 111 (E10), 10–+.
- [5] Smith, M. D., 2004. Interannual variability in TES atmospheric observations in Mars during 1999–2003. *Icarus* 167, 148–165, doi:10.1016/j.icarus.2003.09.010.
- [6] Smith, M. D., Aug. 2009. THEMIS observations of Mars aerosol optical depth from 2002–2008. *Icarus* 202, 444–452.